Adsorption and Corrosion Inhibition Potentials of Salicylaldehyde-based Schiff Bases of Semicarbazide and *p*-Toluidine on Mild Steel in Acidic Medium: Experimental and Computational Studies

Lukman O. Olasunkanmi[a,b], Aishat O. Idris[a], Adetola H. Adewole[c], Olaide O. Wahab[d], and Eno E. Ebenso[b,e]

[a]Department of Chemistry, Faculty of Science, Obafemi Awolowo University, Ile-Ife 220005, Nigeria
[b]Materials Science Innovation & Modelling (MaSIM) Research Focus Area, Faculty of Natural and Agricultural Sciences, North-West University, Private BagX2046, Mmabatho 2735, South Africa
[c]Department of Chemistry, Faculty of Natural and Agricultural Sciences, University of Pretoria, Pretoria 0002, South Africa
[d]Department of Chemistry, Faculty of Pure and Applied Sciences, Nigerian Army University Biu, Nigeria
[e]Institute for Nanotechnology and Water Sustainability, College of Science, Engineering and Technology, University of South Africa, Johannesburg, South Africa

* Corresponding author - E-mail address: waleolasunkanmi@gmail.com (L.O. Olasunkanmi).

Graphical abstract

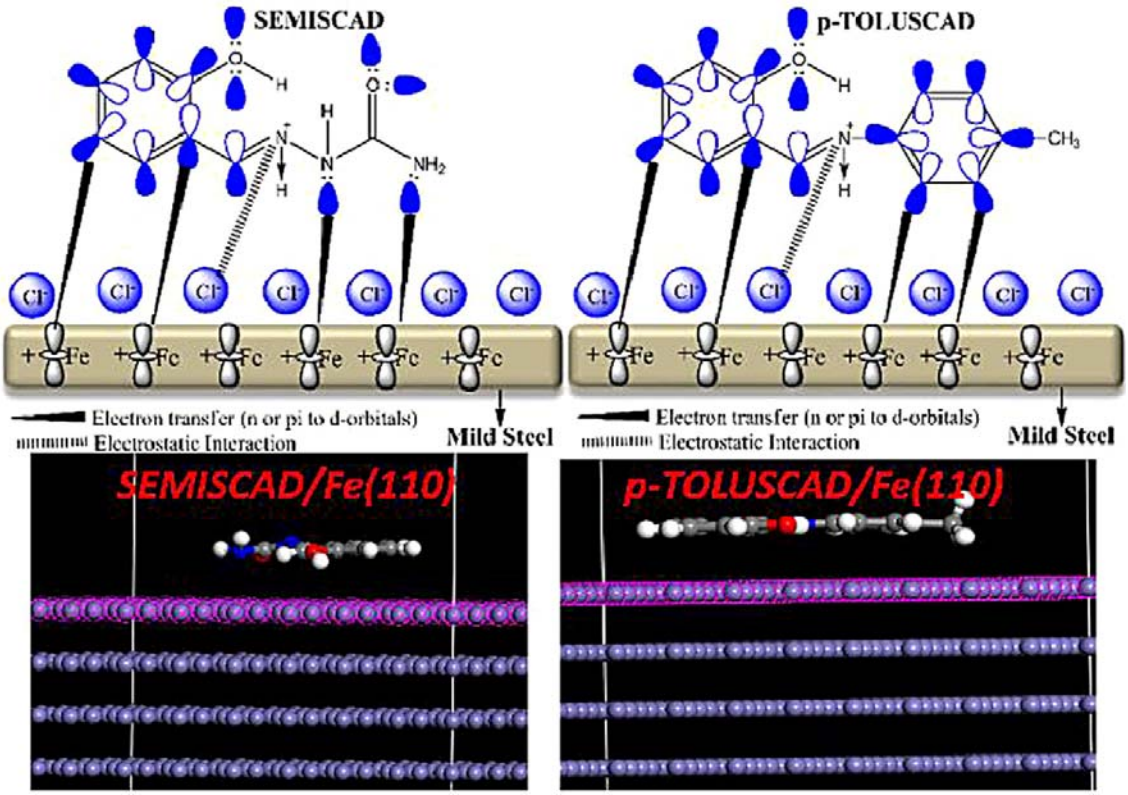

Abstract

Experimental studies, supported by comprehensive density functional theory (DFT) and Monte Carlo simulation studies have been carried out on 2-(2-hydroxybenzylidene) hydrazinecarboxamide (SEMISCAD) and 2-((p-tolylimino)methyl)phenol (p-TOLUSCAD), to describe their corrosion inhibition potentials for mild steel in hydrochloric acid (HCl). The newly synthesized Schiff bases inhibit corrosion of mild steel in 1 M HCl, and their corrosion inhibition efficiencies increase with increase in concentration. Inhibition efficiencies of 79 % and 86 % were obtained for SEMISCAD and *p*-TOLUSCAD, respectively at 303 K and minute concentration (5×10^{-4} M). The results further revealed that p-TOLUSCAD could be an averagely efficient formulation to exhibit 50% inhibition efficiency, even at elevated temperature (343 K). Both compounds were found to inhibit corrosion at the anodic and cathodic sites on the steel, and they are therefore mixed-type inhibitors. Electrochemical impedance spectroscopy (EIS) data revealed the adsorptive nature of the molecules on the steel surface. SEMISCAD and *p*-TOLUSCAD inhibit steel corrosion by adsorbing at steel/HCl interface via physisorption and chemisorption mechanisms. Reactivity parameters predicted from DFT calculations suggested the involvement of protonated forms of the molecules in the inhibitive process, and *p*-TOLUSCAD as a potentially better corrosion inhibitor than SEMISCAD, which is also supported by the adsorption characteristics derived from Monte Carlo simulations.

Keywords: Schiff base; Mild steel; HCl; Tafel Polarization; EIS; DFT; Monte Carlo Simulation

1. Introduction

Corrosion is the spontaneous wearing or deterioration of materials in aggressive media. This process has been of serious concern over the years due to its negative economic and environmental impacts on individuals, industries and nations. It has remained a far-reaching global scientific problem with devastating effects on metallurgical, chemical, food processing, oil industries and even human lives and properties. Consequently, series of studies focusing on corrosion control have been reported [1], [2], [3], [4], [5], [6], [7], [8]. The popularity of mild steel in industrial applications is connected with its high mechanical strength, relatively low cost, availability and weldability, compared to many other alloys. However, steels are highly vulnerable to corrosion in common aqueous environments, and the corrosion rate is particularly high in acidic pHs [9,10].

A comparative analysis of cost and efficiencies of known corrosion control methods puts the use of corrosion inhibitors at a rational edge [11]. An inhibitor forms a protective film at electrode/electrolyte interface, thereby reducing interfacial interactions between a metal (the electrode) and aggressive electrolyte ions. The protective film of an inhibitor on metal surface reduces the rate of metal dissolution in the corrosive medium [12]. Adsorption mechanism of an inhibitor may vary with several factors, such as concentration, pH, nature of the acid anion, nature of the metal, chemical substituents and functional group present, as well as the size of the aromatic and aliphatic moieties of the inhibitor molecule [13]. Thus, it is often not possible to assign a single general mechanism to an inhibitor.

Despite their successes in corrosion control, the negative environmental impacts of inorganic inhibitors such as chromates, dichromates, phosphates, nitrites, and nitrates remain a huge demerit. The environmental unfriendliness and bio-toxicity of these compounds, especially

chromates, are well documented [14,15]. Thus, the quest for a less toxic, more effective and environmentally noble corrosion inhibitors has been on the increase in recent time. Organic corrosion inhibitors seems to be more promising towards achieving an eco-friendly and effective prevention of mild steel corrosion [1,2,5,16]. Besides the possibility of formulating organic corrosion inhibitors from relatively cheap and eco-friendly materials, their utilization proffers a relatively more convenient and effective approach to suppressing metal corrosion and dissolution [17,18].

The compositional features of organic compounds with probable corrosion inhibition activities include the presence of principal heteroatoms such as nitrogen (N), phosphorus (P), sulfur (S) and oxygen (O), and the presence of π-electrons and/or polar functional groups such as –OH, >C=O, –CN, $–NH_2$, $–CONH_2$ etc., which promote donor-acceptor interactions between inhibitor molecules and metallic atoms [4].

The presence of polar imine functional group couple with beneficial biological activities have favoured Schiff bases to be a large family of organic compounds often explored in the quest for environmentally benign corrosion inhibitors [19], [20], [21]. Though, not many reports have been documented on the corrosion inhibition characteristics of salicylaldehyde-based Schiff bases, a few studies on some compounds of this descent have demonstrated their potentials to inhibit metal corrosion [7,22,23].

In furtherance of research exposition on corrosion inhibition properties of Schiff bases, the present study reports the inhibition potentials of 2-(2-hydroxybenzylidene)hydrazine-carboxamide (SEMISCAD) and 2-((*p*-tolylimino)methyl)phenol (*p*-TOLUSCAD) (Fig. 1) on mild steel corrosion in 1 M HCl.

2-(2-hydroxybenzylidene)hydrazinecarboxamide (SEMISCAD)

2-((p-tolylimino)methyl)phenol (p-TOLUSCAD)

Figure 1. 2D molecular structures of SEMISCAD and p-TOLUSCAD.

2. Experimental Details

2.1. Synthesis of 2-(2-hydroxybenzylidene)hydrazinecarboxamide [SEMISCAD] and 2-((p-tolylimino)methyl)phenol) [*p*-TOLUSCAD]

For the synthesis of SEMISCAD, semicarbazide hydrochloride was first mixed with excess potassium carbonate (K_2CO_3), after which the resulting solution was mixed with equimolar quantity (0.0025 mol) of salicylaldehyde. In the case of p-TOLUSCAD, equimolar quantities (0.0025 mol) of salicylaldehyde and p-toluidine were mixed. In each case, the mixture of aldehyde and amine was irradiated in microwave oven for about 3 min and allowed to cool. The observed products were then recrystallized in ethanol.

The synthesized compounds were characterized using melting point determination and nuclear magnetic resonance (NMR) spectroscopic technique.

2.2. Preparation of Corrosive Electrolyte Media

The control corrosive electrolyte solution of 1 M HCl was prepared by appropriately diluting the stock solution of the acid (37% HCl) with distilled water. Inhibitor-containing solutions were prepared in 1 M HCl. Meanwhile, to ensure uniform dissolution of the Schiff bases used, the compounds were first dissolved in 5 mL ethanol before making up each to 1 L solution with 1 M HCl for a 1000 µM (taking as the stock) concentration of the inhibitors. Various concentrations of the inhibitors (100 µM – 500 µM) were prepared from the stock by serial dilution using 1 M HCl.

2.3. Composition of Tested Alloy and Surface Pre-treatment

The tested alloy (mild steel) is composed of essentially Fe (ca. 99.70%), and trace quantities of other elements (in weight percent), i.e. C (0.17), Mn (0.46), Si (0.26), S (0.017), and P (0.019). The surface of each mild steel sample was pre-treated by abrading it with silica carbide paper of graded grit sizes (600 – 1200), before washing with water, degreased in acetone and dried in hot air.

2.4. Gravimetric or Weight-Loss Experiment

The appropriateness of weight-loss method in terms of its operational simplicity and good reliability for corrosion inhibition studies is well known [1,2,4, 5, 24]. For this experiment, surface pre-treated metal coupons of a fixed dimension (1 cm by 8 cm) were pre-weighed before immersing in the test solutions for 3 h. The specimens were removed after the elapsed time, gently brushed and rinsed with water to remove loosely bound corrosion products, degreased in acetone and dried in warm air, and then re-weighed. This process was carried out for different concentrations of both SEMISCAD and p-TOLUSCAD and at different temperatures (40°C, 50°C, 60°C, 70°C). The weight-loss for each experiment was recorded (in triplicates) and the inhibition efficiency (%I$_W$) and corrosion rate (C_R) (in mgcm^{-2}s^{-1}) were computed using as [25]:

$$\%I_W = \frac{w^0 - w}{w^0} \times 100 \quad (1)$$

$$C_R = \frac{W_N - W_0}{At} \quad (2)$$

where w^0 and w represent the weight-loss values (average of triplicate measurements) obtained without and with various inhibitor concentrations; W_0 and W_N are the weights in grams (average of triplicate measurements) of mild steel before and after immersion into the corrosive media; A is the exposed surface area in cm^2; and t is time in seconds.

2.5. Electrochemical Experiments

These experiments were carried out only at room temperature, just to have gain some insights into the electrochemical behaviour of the electrode/electrolyte systems being studied. The measurements were conducted in a glass cell equipped with the working, reference and counter electrodes. The working electrode (WE) is a mild steel coupon of 1 cm x 1 cm square dimension that has been covered with epoxy resin at one side, exposing only one side with 1

cm^2 surface area. A Ag/AgCl, 3 M KCl was used as the reference electrode (RE), while a platinum plate was used as the counter electrode (CE).

For the potentiodynamic polarization experiments, the electrochemical cell was connected to a PG581 potentiostat/galvanostat (from Biologic, France). The open-circuit potential (OCP) of the WE in each test solution was monitored for 30 min, within which a relatively stable OCP was assumed by the electrode. The potential of the WE was polarized (potentio-dynamically) between -250 mV and +250 mV, relative to the OCP at the ASTM-recommended scan rate of 0.167 mV/s. The polarization curves were analyzed using the corrosion fitting codes implemented in UiEcorr (version 3.08) software from Uniscan Instruments. Electrochemical parameters, such as corrosion potential (E_{corr}), corrosion current density (i_{corr}), anodic (β_a) and cathodic (β_c) Tafel slopes were derived from the analyses. Percentage inhibition efficiencies (%I_P) were calculated as [26]:

$$\%I_P = \frac{i_0 - i_i}{i_0} \times 100 \quad (3)$$

where i_0 and i_i are corrosion current densities in the absence and presence of inhibitors, respectively.

For the electrochemical impedance spectroscopy (EIS) experiments, CorrTest potentiostat equipped with CS Studio5 software (ver. 5.3) was used. The experiments were conducted at the OCP by analyzing the response of mild steel electrode (1 cm^2 surface area) in the electrolyte media to the passage of alternating current in the frequency range of 10^{-2} Hz to 10^5 Hz at 10 mV amplitude.

2.6. Density Functional Theory (DFT) Calculations

DFT calculations were performed using Gaussian 09W (revised version D.01) [27]. SEMISCAD and *p*-TOLUSCAD molecules were modelled with GaussView 5.0 and subjected to full optimization without symmetry constraints to obtain the ground state minimum energies and geometries both in the gas phase and HCl medium. Calculations in HCl medium were carried out by treating the solvent medium with IEPCM, and the HCl medium was defined as having static and optical dielectric constants of 78.3 and 1.573 respectively as described elsewhere [6]. All optimized geometries were confirmed to have no negative vibrational frequencies. All the calculations were carried out with the B3LYP/6-31+G(d,p) model [28]. The relative potentials of both compounds to inhibit corrosion were traced to their chemical reactivity using some selected reactivity parameters, such as energy gap (ΔE), global hardness (η), electronegativity (χ) and electrophilicity (ω) which were estimated from the HOMO and LUMO energies of the optimized molecules using the following equations [1,29,30]:

$$\Delta E = E_{LUMO} - E_{HOMO} \quad (4)$$

$$\eta = \frac{1}{2}(E_{LUMO} - E_{HOMO})$$
$$\chi = -\frac{1}{2}(E_{HOMO} + E_{LUMO}) \quad (5)$$

$$\omega = \frac{\chi^2}{2\eta} \quad (6)$$

2.7. Monte Carlo Simulations

Since the major mode of corrosion inhibition by organic molecules is adsorption on metallic surface, adsorption of SEMISCAD and p-TOLUSCAD molecules on mild steel surface was mimicked by using the Monte Carlo simulation approach. Mild steel being essentially Fe was represented by Fe(110) crystal surface. Fe(110) plane was used because of its favorable atomic density and energetics [2,31,32]. Fe(110) crystal surface was modelled by cleaving the metallic Fe, which was then optimized using the Forcite force field. The optimized Fe(110) was made into a 10 × 10 supercell and multiple layers in 15 Å vacuum slab. The inhibitor molecule was made to approach the Fe(110) surface by invoking the adsorption locator module available in Materials Studio 2018 software suite. COMPASS force field and smart algorithm were used for the simulated annealing process [16].

3. Results and Discussion

3.1. Synthesis and Characterization

Both SEMISCAD and p-TOLUSCAD were synthesized and the characterization results are summarized in Table 1. The ^{1}HNMR and ^{13}CNMR spectra of the compounds are presented in Figures S1 and S2, respectively in the Supplementary Information. For diagnostic purposes, special mentions are made (from Table 1 and Figures S2) of the appearances of the expected 8 and 12 distinct carbon peaks in the ^{13}C-NMR spectra of SEMISCAD and p-TOLUSCAD respectively. Similarly, the ^{1}H-NMR spectra of the two compounds also showed the expected proton peaks. Furthermore, the characterization results in Table 1 are in agreement with literature reports on SEMISCAD [33], [34], [35] and p-TOLUSCAD [36], [37], [38], [39], suggesting the successful synthesis of the two compounds.

Table 1. IUPAC name, molecular structures, molecular formula, molecular weight, melting point and spectroscopic data of the synthesized compounds.

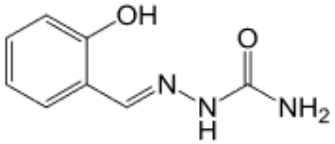	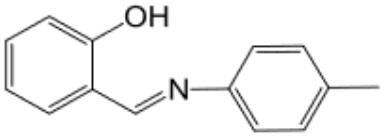
2-(2-hydroxybenzylidene) hydrazinecarboxamide (**SEMISCAD**): Mol. Formula: $C_8H_9N_3O_2$; Mol. wt. 179; Colour: Off-white crystal; Melting Point: 229 – 231°C. ^{1}H NMR δ ppm (400 MHz, DMSO-d6) δ_H 10.19 (1H, *s*, -OH), 9.97 (1H, *s*, -NH), 8.14 (1H, *s*, CH=N), 6.39 (2H, *s*, -NH_2), 6.79 – 7.75 (4 aromatic protons) ^{13}C NMR δ ppm (75 MHz, DMSO-d6) δ_C 156.6 (C-OH), 155.8 (>C=O), 137.4 (C=N), 115.9 – 130.1 (5 aromatic carbons).	2-((p-tolylimino)methyl)phenol (***p*-TOLUSCAD**): Mol. Formula: $C_{14}H_{13}NO$; Mol. wt. 211; Colour: Yellow crystal; Melting Point: 90 – 92°C. ^{1}H NMR δ ppm (400 MHz, DMSO-d6) δ_H 13.22 (1H, *s*, -OH), 8.94 (1H, *s*, CH=N), 6.94 – 7.64 (8 protons on both aromatic rings) 2.33 (3H, *s*, -CH_3) ^{13}C NMR δ ppm (75 MHz, DMSO-d6) δ_C 162.5 (C=N), 160.2 (C-OH), 145.3 (C-N), 116.5 – 136.5 (8 carbons on both aromatic), 20.5 (-CH_3)

3.2. Weight Loss Measurements

3.2.1. Effect of Inhibitor Concentration

The loss in weight of mild steel, the inhibition efficiency (%I_w), and the surface coverage (θ) obtained at various concentrations of the inhibitors are presented in Table 2 for the experiments conducted at 30°C only. The continuous decrease in weight loss as concentrations of SEMISCAD and p-TOLUSCAD might be due to increase in surface coverage, which can be associated with increased number of molecules of the inhibitors that adsorbed on the steel surface, thereby covering the active sites. Therefore, the protection efficiencies of the studied inhibitors increase with increasing concentrations.

Table 2. Weight loss, inhibition efficiency, surface coverage, and corrosion rate obtained for mild steel in 1 M HCl without and with various concentrations of SEMISCAD and *p*-TOLUSCAD at 30°C.

Inhibitor	Conc.(μM)	Weight loss in (mg)	Inhibition efficiency (%I_w)	Surface (Θ) coverage
BLANK	0	70.03±0.12	-	
SEMISCAD	100	57.00±0.08	18.61±0.04	0.19
	200	43.01±0.27	38.58±0.25	0.39
	300	30.20±0.23	56.88±0.61	0.57
	400	20.04±0.17	71.38±0.62	0.71
	500	15.01±0.11	78.57±0.59	0.79
p-TOLUSCAD	100	50.02±0.09	28.57±0.07	0.29
	200	40.11±0.34	42.72±0.37	0.43
	300	25.98±0.06	62.90±0.18	0.63
	400	18.33±0.10	73.83±0.42	0.74
	500	10.08±0.04	85.61±0.37	0.86

The inhibition efficiencies of SEMISCAD and *p*-TOLUSCAD at 500 μM were 79% and 86%, respectively, showing that *p*-TOLUSCAD is a more efficient inhibitor than SEMISCAD. This may be partly due to larger molecular area of *p*-TOLUSCAD, contributed by the molecular size of aromatic rings, and extended pi-electrons that might favour adsorption of the molecules on metallic surface. The combined effects of larger molecular area and aromatic pi-electrons in *p*-TOLUSCAD might favour its adsorption on metallic surface better than the increased number of hetero-atoms in SEMISCAD.

3.2.2. Effects of Temperature Variation on Inhibition Potentials of SEMISCAD and p-TOLUSCAD

The effects of temperature variation on the inhibition potentials of SEMISCAD and *p*-TOLUSCAD on corrosion of mild steel in 1 M HCl were investigated at 500 μM, and the results are plotted in Figure 2. As shown in Figure 2a, the rate of mild steel corrosion (C_R) in the acid increases progressively from 30°C to 70°C, both in the absence and presence of the inhibitors. The inhibition efficiencies (%I_W) of both SEMISCAD and *p*-TOLUSCAD decrease with increase in temperature. Since temperature increases the kinetic energy of an ion/molecule, the increase in C_R with increase in temperature can be attributed to increased collision rate between the aggressive/corrosive acidic ions and mild steel. In addition to this view which holds in the absence of inhibitor molecules, the increase in C_R with increase in temperature in the presence of inhibitor molecules can be ascribed to desorption of already adsorbed inhibitor molecules.

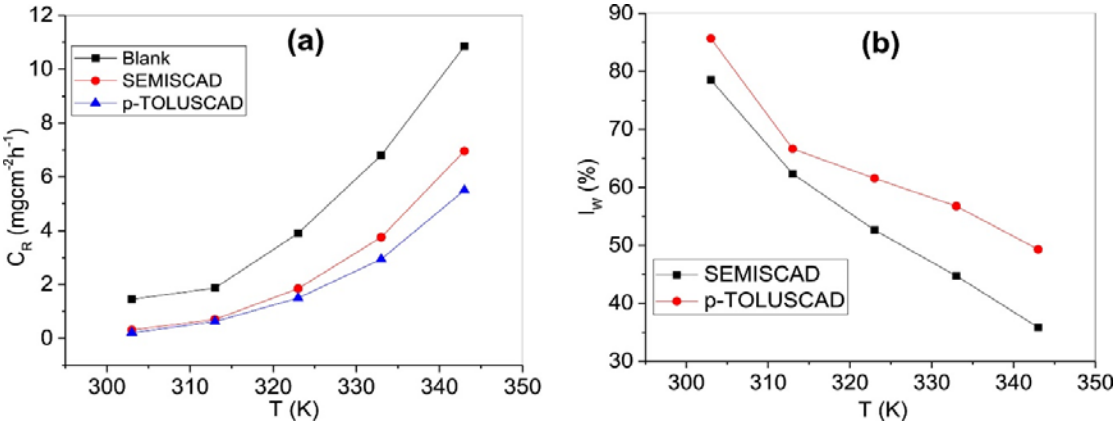

Figure 2. Variation of corrosion rate (C_R) **(a)**, and inhibition efficiency (%I_W) **(b)** with temperature for 500 µM concentration of the inhibitors.

The order of the %I_W for the two compounds over the studied temperature range is *p*-TOLUSCAD > SEMISCAD, with *p*-TOLUSCAD showing 49% and SEMISCAD showing 36% inhibition efficiencies at 70°C.

The C_R-T data were fitted into the Arrhenius equation of the form:

$$log\ (C_R) = \frac{-E_a}{2.303RT} + log\ A \tag{8}$$

where E_a represents activation energy, R is the molar gas constant, T is the temperature and A represents the pre-exponential factor. The Arrhenius plots for reactions are shown in Figure 3a. The activation energies obtained from the slopes ($-E_a$/2.303R) of the respective Arrhenius plots are listed in Table 3 where the trend of the values of E_a is in the order *p*-TOLUSCAD (30.48 kJ/mol) > SEMISCAD (29.61 kJ/mol) > Blank (19.86 kJ/mol). This implies that the energy barrier to the corrosion process is higher and the rate of corrosion is lowered in the presence of the inhibitors. The inhibitor molecules probably form protective layers on the mild steel surface thereby reducing its rate of dissolution in the corrosive medium.

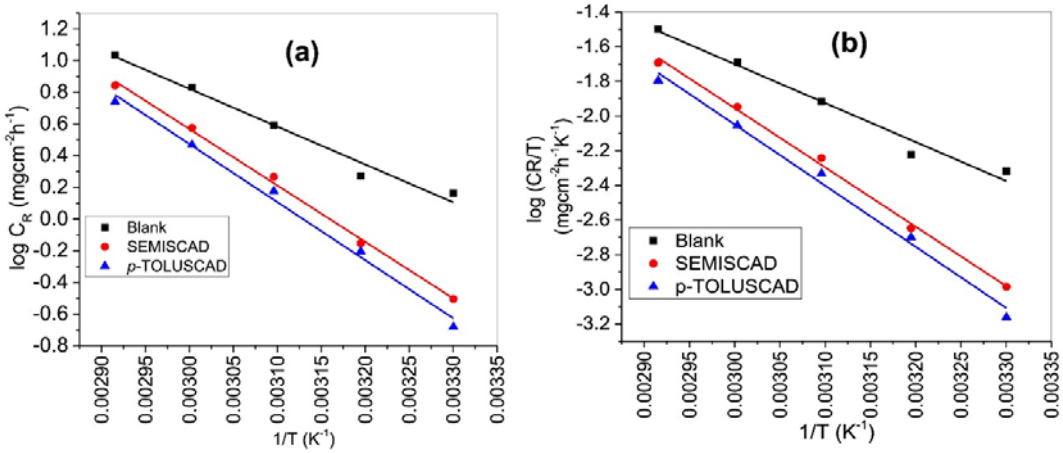

Figure 3. Arrhenius **(a)** and transition state **(b)** plots for the corrosion of mild steel in 1 M HCl without and with 500 µM of SEMISCAD and *p*-TOLUSCAD.

Table 3. Activation energies (E_a), activation enthalpies (ΔH*) and activation entropies (ΔS*) for mild steel corrosion in 1 M HCl in the absence and presence of 500 µM of SEMISCAD and *p*-TOLUSCAD.

INHIBITOR	E_a (kJ/mol)	ΔH* ($kJmol^{-1}$)	ΔS* ($Jmol^{-1}K^{-1}$)
Blank	19.86	43.06	-100.94
SEMISCAD	29.61	65.51	-38.45
p-TOLUSCAD	30.48	67.51	-34.27

To further describe the transition state behaviour of the adsorption/desorption process involved in mild steel corrosion in the studied media, the C_R-T data were fitted into the transition state equation of the form [40]:

$$\log\left(\frac{C_R}{T}\right) = \left[\log\left(\frac{R}{Nh}\right) + \left(\frac{\Delta S^*}{2.303R}\right)\right] - \frac{\Delta H^*}{2.303\,RT} \quad (9)$$

where ΔH^* and ΔS^* represent enthalpy and entropy of activation, respectively, h is the Planck's constant and N is Avogadro's constant. The ΔH^* and ΔS^* values were calculated from the slope and intercept of the plots of log C_R/T against 1/T, which are shown in Figure 3b, and the results obtained are also listed in Table 3.

The positive values of ΔH* in Table 3 indicate that the formation of activated complex during the corrosion process is endothermic [5]. The values of ΔH* in the presence of the inhibitors revealed high-energy activated complexes that can readily transform to a steel-inhibitor complex. The negative ΔS* values suggest that the activated-complex formation step is an associative process which lowers the entropy of the system through production of a more ordered species. The higher values of ΔS* compared to the blank are indications of the involvement of larger molecules/species in the activated complexes of the inhibitor-containing process than those (water and oxides) involved in the absence of the inhibitors. The entropy of activation increases as water molecules are desorbed from the steel surface while the inhibitor molecules are being adsorbed onto the surface. Since the rate determining step is the discharge of hydrogen ions to form adsorbed hydrogen atoms [5], the presence of inhibitor molecules on the steel surface will therefore slow down the discharge of hydrogen ions at the metal surface causing increased disorderliness in the system, and hence, relatively high entropy of activation.

3.3. Adsorption Isotherms

The major mechanism by which organic molecules inhibit metal corrosion is through adsorption onto the metallic surface. A better understanding of corrosion inhibition mechanism is often sought from the point of view of adsorption isotherms. In view of this, the adsorption behaviors of SEMISCAD and *p*-TOLUSCAD on mild steel surface were investigated by treatment of the experimental surface coverage data (Table 1) with different adsorption models, which include Langmuir, Freundlich and Temkin, isotherms. The correlation coefficient (R^2) values indicate that the adsorption of the studied inhibitors on the steel surface in 1 M HCl solution obeys the Temkin adsorption isotherm model. A linear form of the isotherm is [41,42]:

$$\theta = \left(-\frac{1}{2a}\right) lnK_{ads} + \left(-\frac{1}{2a}\right) lnC \quad (10)$$

where θ is the surface coverage, C is inhibitor concentration, K_{ads} is adsorption equilibrium constant, and "a" is the molecular interaction parameter. The change in Gibb's free energy (ΔG_{ads}) of adsorption was determined from K_{ads} value using the relation:

$$\Delta G_{ads} = -RTln\,(55.5K_{ads}) \quad (11)$$

where R is gas constant, T is absolute temperature and 55.5 is the molar concentration of water in the bulk solution [5].

The Temkin adsorption isotherms are shown in Figure 4. The adsorption parameters and the derived ΔG_{ads} values are listed in Table 4. The results suggest that both SEMISCAD and *p*-

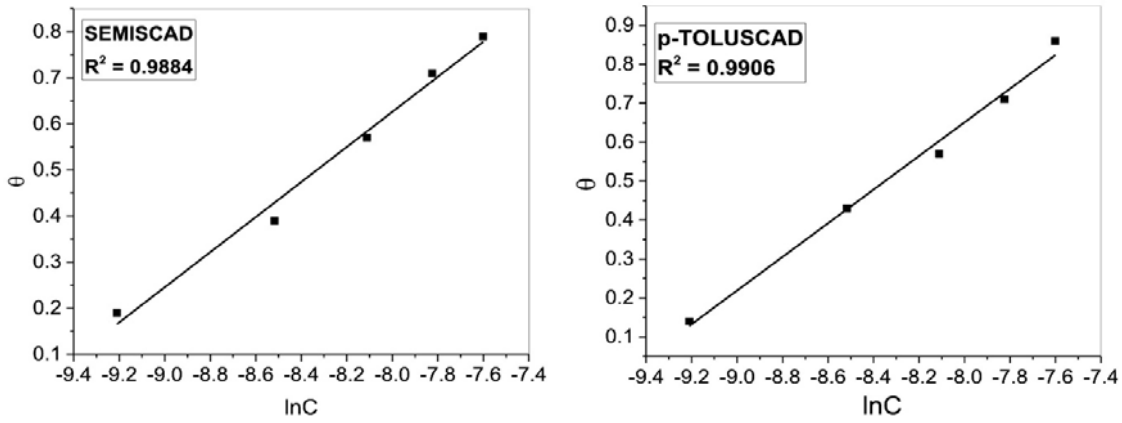

Figure 4. Temkin isotherm plots for the adsorption of SEMISCAD and p-TOLUSCAD at steel/HCl interface.

Table 4. The values of K_{ads} and ΔG_{ads} for the adsorption of *p*-TOLUSCAD and SEMISCAD on mild steel in 1 M HCl at 303 K.

INHIBITORS	K_{ads} (x10^4)	$-a$	$-\Delta G_{ads}$ (kJ/mol)
SEMISCAD	1.55	1.31	34.42
p-TOLUSCAD	1.35	1.16	34.07

TOLUSCAD molecules have favourable adsorption at the steel/HCl interface. Though a slightly larger value of K_{ads} was obtained for SEMISCAD, compared to *p*-TOLUSCAD, the molecular interaction parameters suggest more intermolecular repulsion at the adsorption layers of SEMISCAD compared to *p*-TOLUSCAD. The values of ΔG_{ads} for the two compounds also suggest the interplay of physical and chemical adsorption mechanisms [43].

3.4. Electrochemical Measurements

3.4.1. OCP-time profile and potendiodynamic polarization measurements

The open circuit potential (OCP) profiles of the corrosion of mild steel in the studied media were recorded from 0 min to 30 min and the plots are shown in Figure 5a. The profile revealed that the electrochemical systems attained a relatively steady potential within 30 min of steel immersion in the electrolytes. The electrode potentials in the presence of the inhibitors are more cathodic than that of the blank, suggesting that the inhibitive effects of the compounds are more pronounced on the cathodic half-reaction of the corrosion process.

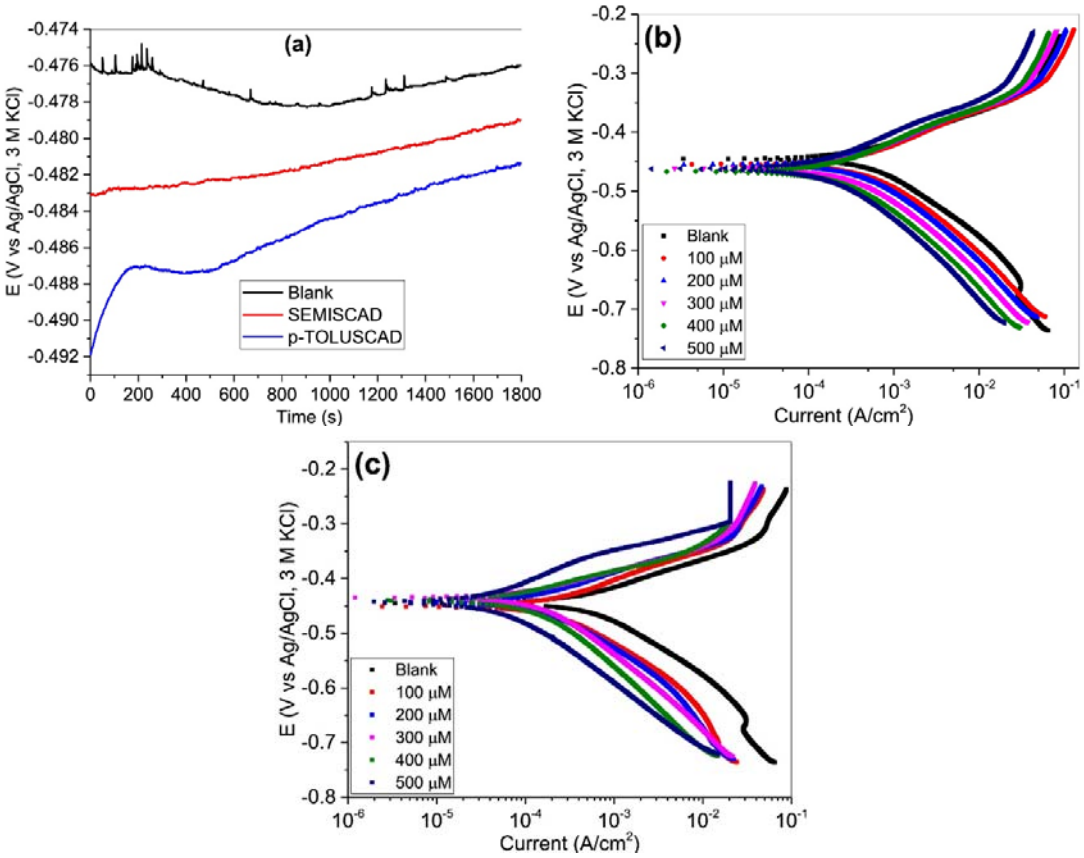

Figure 5. OCP-time Profiles for mild steel in 1 M HCl (without inhibitor, i.e. the blank), and systems containing 500 µM SEMISCAD and p-TOLUSCAD **(a);** and potentiodynamic polarization curves for mild steel in 1 M HCl without and with different concentrations of **(b)** SEMISCAD and **(c)** p-TOLUSCAD, at room temperature.

Table 5. Potentiodynamic polarization parameters for mild steel in 1 M HCl in the absence and presence of different concentrations of the studied inhibitors at room temperature.

Inhibitor Concentration (µM)	$-E_{corr}$ (mV*)	β_a (mV/dec)	$-\beta_c$ (mV/dec)	i_{corr} (µA/cm²)	% I_P
Blank					
0	439	62	130	93	-
SEMISCAD					
100	453	64	141	73	21
200	454	66	145	53	43
300	458	66	143	36	61
400	463	60	147	28	70
500	462	67	151	18	81
***p*-TOLUSCAD**					
100	450	58	125	62	33
200	443	63	119	54	42
300	433	50	128	32	66
400	439	55	120	22	76
500	443	51	133	9	90

*E_{corr} was recorded in mV vs Ag/AgCl, 3 M KCl

Potentiodynamic polarization curves for mild steel in 1 M HCl without and with different concentrations of SEMISCAD and *p*-TOLUSCAD at room temperature are shown in Figures 5b and 5c, respectively. The curves are shifted to lower current region by the addition of the inhibitors. The cathodic arms of the curves appear at orderly decreased current regions with increasing concentration of the inhibitors, suggesting that the cathodic hydrogen gas evolution reaction is essentially controlled by the increasing amount of the inhibitor molecules. Electrochemical corrosion parameters such as corrosion potential (E_{corr}), anodic and cathodic Tafel slopes (β_a and β_c, respectively), and corrosion current density (i_{corr}) were obtained by extrapolating the linear portions of the anodic and cathodic polarization curves to the corrosion potential. The results are presented in Table 5 along with the corrosion inhibition efficiency (%I_P) values which were calculated from i_{corr} using Equation 2.

The results showed a decrease in i_{corr} value from the blank to the inhibitor-containing acid solution. The i_{corr} value decreases with increase in inhibitor concentration and this is accompanied by a slight shift in E_{corr} value. An inhibitor is classified as anodic inhibitor if the shift in E_{corr} value relative to the blank is above 85 mV in the direction of the anode, cathodic if the shift is above 85 mV in favor of the cathode, and mixed-type if the shift is less than 85 mV [16,27]. There is only a slight difference between the E_{corr} of the blank and inhibitor-containing systems (as shown in Table 5). This suggests that the studied compounds are mixed-type corrosion inhibitors, inhibiting both the anodic dissolution of mild steel and the cathodic evolution of hydrogen gas. The inhibitors reduce the corrosion current density (i_{corr}), and the values of i_{corr} at the maximum concentration of the inhibitors are in the order *p*-TOLUSCAD < SEMISCAD. The order of inhibition efficiencies of the compounds is *p*-TOLUSCAD > SEMISCAD, which is agreement with the observed trend of inhibitive potentials from the weight-loss measurements (Table 2).

3.4.2. Electrochemical impedance spectroscopy (EIS) measurements

The results of EIS measurements are presented as Nyquist and Bode plots in Figure 6, Figure 7 respectively. The Nyquist plots exhibit depressed capacitive loop that results in imperfect semicircular profiles. This feature has been described as frequency dispersion phenomenon that is characteristic of solid electrode systems, and it is associated with roughness and inhomogeneity of electrode surface [44]. The single capacitive loop in the Nyquist plots together with the appearance of only one time-constant in the Bode plots suggests that the studied compounds behave as interfacial inhibitors and mitigate mild steel corrosion in the studied electrolyte via simple surface coverage [45]. The diameter of the Nyquist plots increases with increasing concentration of the inhibitors, suggesting that the inhibition potentials of the compounds have direct relationship with the amount of the Schiff bases in solution. The increase diameter of the Nyquist plots is indicative of increased impedance to the follow of charges across steel/electrolyte interface. A reduced charge transfer process implies a reduced corrosion rate. In addition, it was observed that the EIS profiles show no significant difference between the blank and inhibitor-containing systems, which suggests that the addition of the studied inhibitors does not alter the corrosion mechanism of mild steel in 1 M HCl. This further corroborates the fact the molecules inhibit the corrosion of steel by simple surface coverage.

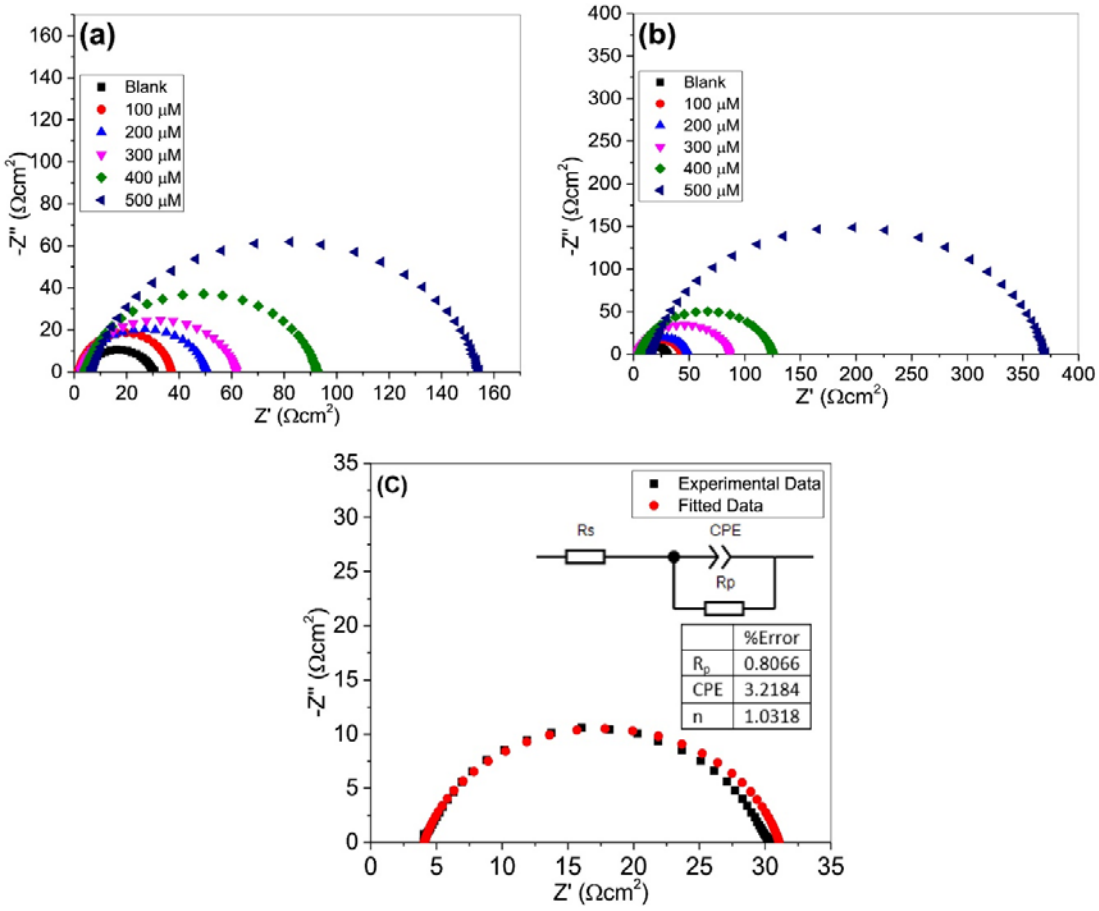

Figure 6. Nyquist plots for mild steel in 1 M HCl in the absence and presence of different concentrations of **(a)** SEMISCAD, **(b)** p-TOLUSCAD, and **(c)** representative fitting regime for the blank experiment, showing equivalent circuit and percentage errors.

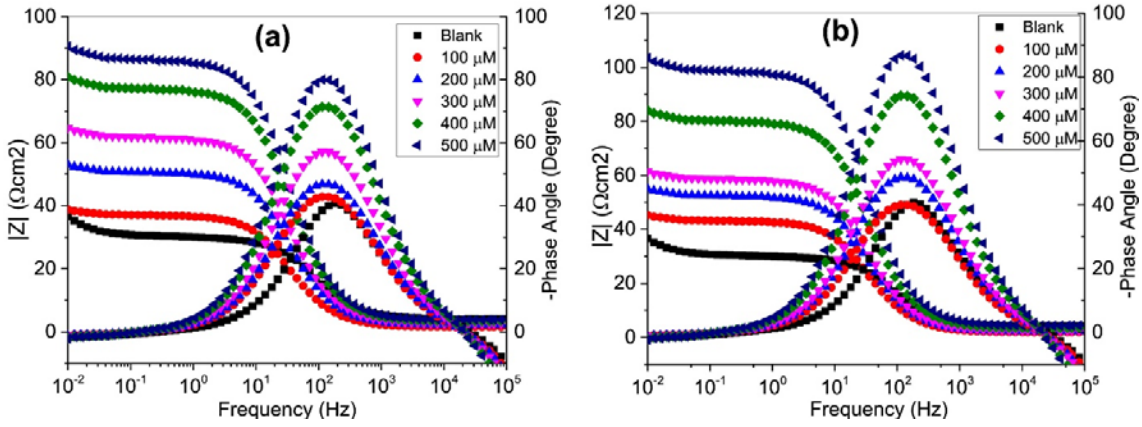

Figure 7. Bode plots for mild steel in 1 M HCl in the absence and presence of different concentrations of **(a)** SEMISCAD, and **(b)** p-TOLUSCAD.

The EIS spectra were analyzed with the CS Studio5 (ver. 5.3) fitting codes by using the equivalent circuit shown as an inset in Figure 6c. The overlaid experimental and fitted data in Figure 6c and the residual percentage errors showed that the adopted equivalent circuit is

suitable for simulating the experimental data. The inclusion of constant phase element (CPE) in the circuit is to ensure a good fit of the experimental data and proper description of the adsorptive behaviour of the inhibitor molecules. The CPE impedance can be described by the equation [1,44, 45]:

$$Z_{CPE} = Y_o^{-1}(j\omega)^{-n} \tag{12}$$

where Y_o is the CPE or proportionality constant, j is the imaginary number, ω is the angular frequency, and n is a CPE exponent or phase shift. The double layer capacitance were determined from the relation [44]:

$$C_{dl} = Y_o(\omega_{max})^{n-1} \tag{13}$$

The percentage inhibition efficiency (%I_I) was estimated from the polarization/charge transfer resistance (R_P) as:

$$\%I_I = 100\left(1 - \frac{R_p^o}{R_p^i}\right) \tag{14}$$

where R_p^o and R_p^i are the charge transfer/polarization resistances for the blank and inhibitor-containing systems respectively.

Table 6. EIS parameters for mild steel in 1 M HCl in the absence and presence of different concentrations of the studied inhibitors at room temperature.

Inhibitor Concentration (μM)	R_p (mV/dec)	C_{dl} (μF/cm^2)	n	$\%I_I$
Blank				
0	26.60	257.19	0.77	
SEMISCAD				
100	35.43	180.03	0.79	24.91
200	48.42	167.17	0.80	45.06
300	59.04	136.31	0.83	54.95
400	88.56	115.74	0.85	60.00
500	147.61	90.02	0.84	81.98
p-TOLUSCAD				
100	41.33	159.71	0.82	35.64
200	47.23	125.25	0.85	43.69
300	82.66	92.33	0.88	67.82
400	119.86	80.76	0.87	77.81
500	354.26	77.67	0.89	92.49

The EIS parameters derived from the fitting regime are listed in Table 6. The values of R_p and also %I$_I$ increase with increasing concentrations of SEMISCAD and p-TOLUSCAD. The results showed higher values of %I$_I$ for p-TOLUSCAD than SEMISCAD, which is in agreement with the observed results from polarization measurements. The values of C_{dl} for the inhibitor-containing systems are lower than that of the blank, which suggests the presence of double layer capacitive film at the electrode/electrolyte interface in the presence of inhibitors. The decreasing values of C_{dl} with increasing concentration of the inhibitors is due to increasing thickness of the double layer formed by the adsorbed film of the inhibitor molecules. The closer values of n (in Table 6) to unity in the presence of inhibitor molecules

is another indication of adsorbed film of inhibitor molecules on the steel surface and suggests pseudo-capacitive behaviour of the interface.

Though direct comparison of performances of organic corrosion inhibitors is difficult to generalize because many factors are at play, a quick glance at the literature revealed relative performances of the studied compounds compared to few others previously reported. The inhibition efficiencies of some Schiff bases that had been assessed as corrosion inhibitors for mild steel in 1 M HCl using EIS method are listed in Table 7 alongside the studied compounds. The data in Table 7 show that the studied compounds also perform reasonably well as corrosion inhibitors in the family of Schiff bases that have been investigated for similar application.

Table 7. Comparative list of corrosion inhibition efficiencies (at 500 μM) of some Schiff bases in literature and the studied compounds applied for mild steel in 1 M HCl.

Schiff base	Method	% I_E	Reference
(1Z)-2-oxo-N'-phenyl-N-quinolin-8-ylpropanehydrazonamide	EIS	76	[46]
(1Z)-N'-(4-bromophenyl)-2-oxo-N-quinolin-8-ylpropanehydrazonamide	EIS	85	[46]
N-(2-hydroxyphenyl)salicyaldimine	EIS	86	[22]
N-(2-methylphenyl)salicyaldimine	EIS	91	[22]
N-(2-methoxyphenyl)salicyaldimine	EIS	80	[22]
N-(2-nitrophenyl)salicyaldimine•HCl	EIS	40	[22]
N'-(4-Hydroxybezylidene) nicotinic hydrazine	EIS	71	[47]
N'-(4-methylybezylidene) nicotinic hydrazone	EIS	74	[47]
2-pyridyl-N-(2′-methylaminophenyl) methyleneimine	EIS	87	[48]
2-pyridyl-N-(2′-methylthiophenyl) methyleneimine	EIS	84	[48]
2-pyridyl-N-(2′-methoxyphenyl) methyleneimine	EIS	78	[48]
2-(2-hydroxybenzylidene)hydrazinecarboxamide	EIS	82	This work
2-((p-tolylimino)methyl)phenol	EIS	92	This work

3.5. Density Functional Theory (DFT) Calculations

The ground state optimized structures of SEMISCAD and *p*-TOLUSCAD molecules and their protonated forms in the gas phase are shown in Figure 8. The electron density graphics of their respective highest occupied molecular orbitals (HOMO) isosurfaces are shown in Figure 9, while the corresponding isosurfaces of the lowest unoccupied molecular orbitals are shown in Figure S3 (Supplementary Information). The neutral molecule of SEMISCAD is more planar than *p*-TOLUSCAD, which has the methylbenzene ring of the p-toluidine twisted ca. 40° out-of-plane in reference to the other part of the molecule. However, the protonated form of *p*-TOLUSCAD, i.e. [p-TOLUSCAD-H]$^+$ is more planar than that of SEMISCAD, i.e. [SEMISCAD-H]$^+$. If the inhibition efficiencies of the molecules where to be correlated with their planarity, it could be assumed that the higher inhibition efficiency of p-TOLUSCAD is due to the favorable adsorption of [p-TOLUSCAD-H]$^+$, its more planar protonated form compared to [SEMISCAD-H]$^+$.

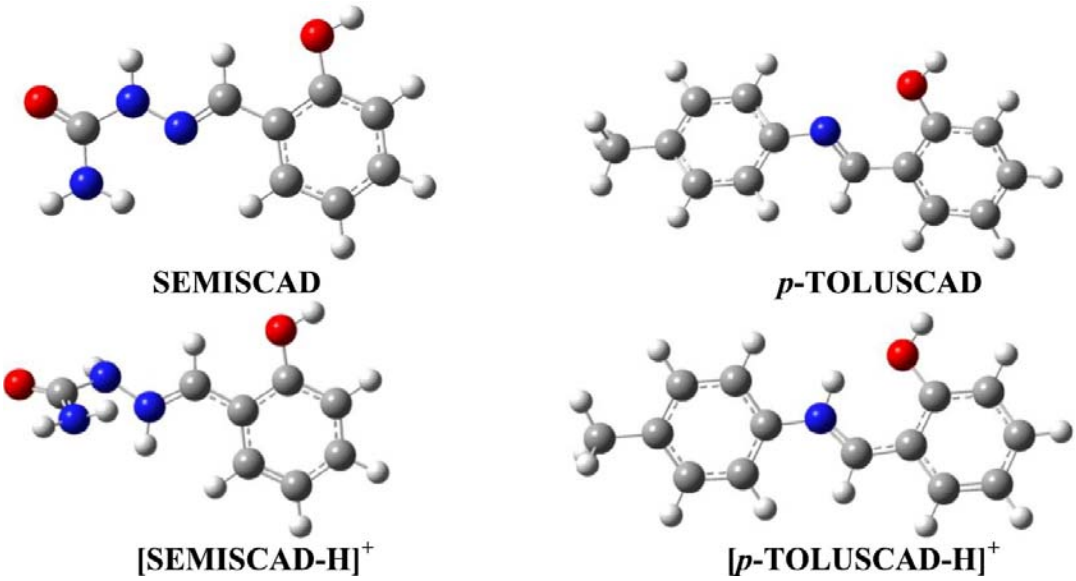

Figure 8. Optimized structures of the neutral and protonated species of the studied molecules (in gas phase). Carbon (grey), Hydrogen (white), Nitrogen (blue) and Oxygen (red).

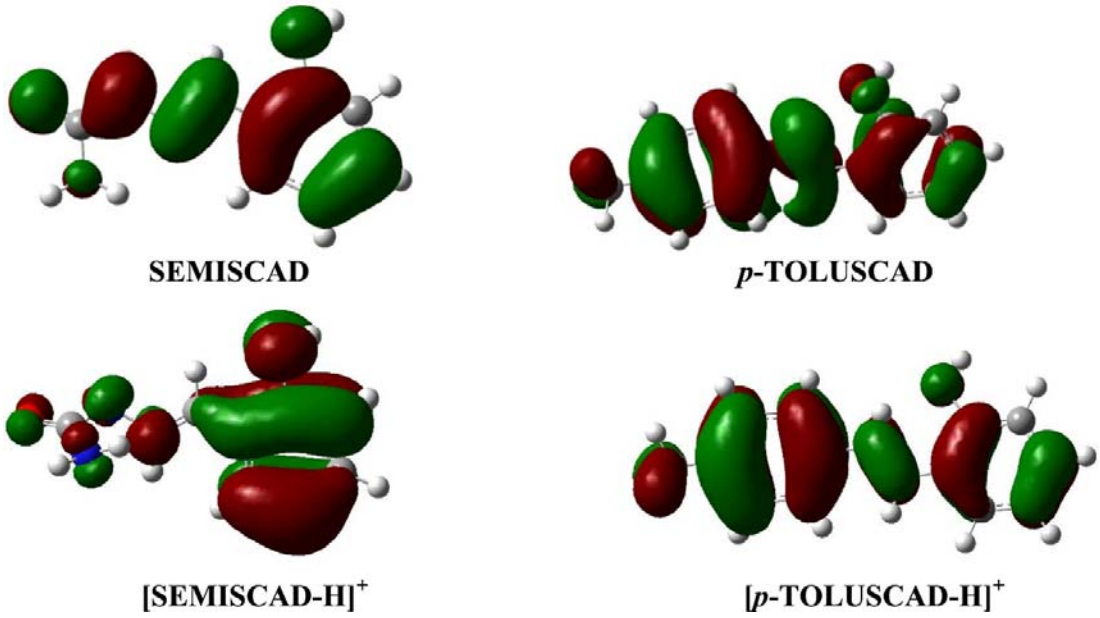

Figure 9. HOMO electron density isosurfaces of the neutral and protonated species of SEMISCAD and *p*-TOLUSCAD (in the gas phase).

The HOMO electron density surface reveals the parts of a molecule with the highest chance of donating electrons into appropriate vacant orbitals of an acceptor. The electron density distribution of the frontier molecular orbitals (Figure 9) showed that the HOMO orbitals of *p*-TOLUSCAD and its protonated form are predominantly of pi-character and the electron density is extended over the entire aromatic system and the pi-electron networks which might favor forward electron donation to the vacant d-orbital of the metal (Fe in mild steel) for donor-acceptor interactions. Since the larger percentage of the electron density of *p*-TOLUSCAD is on the *p*-toluidine, the forward donation from the molecule to vacant d-

orbitals of Fe will most likely come from the *p*-toluidine moiety. SEMISCAD also exhibits a widely distributed HOMO electron density over the entire molecule. However, the HOMO electron density of $[SEMISCAD\text{-}H]^+$ is densely distributed over the salicylaldehyde moiety, suggesting that the adsorption of the molecule on steel surface in acidic medium might be via the aromatic ring. This suggests that the benzene ring will be responsible to a very large extent for electron donation into vacant d-orbitals of Fe.

The quantum chemical reactivity parameters such as energy gap, global hardness, electronegativity and electrophilicity, which were calculated from the HOMO and LUMO energies (i.e. E_{HOMO} and E_{LUMO}, respectively) of the molecules are listed in Table 8. The ability of a molecule to donate or accept electrons can be predicted from its E_{HOMO} and E_{LUMO} values. A molecule with high E_{HOMO} value has a better chance of donating electrons to an acceptor molecule while a molecule with a high E_{LUMO} value has lower tendency of accepting electrons from a donor.

Table 8. Some Quantum Chemical Parameters for the Studied Compounds.

Inhibitor molecule	E_{HOMO} (eV)	E_{LUMO} (eV)	ΔE(eV)	η(eV)	χ(eV)	ω(eV)	Dipole Moment(Debye)
Gas phase							
SEMISCAD	-6.101	-1.790	4.311	2.155	3.945	3.611	5.660
$SEMISCAD\text{-}H^+$	-10.974	-7.213	3.762	1.881	9.093	21.982	5.979
p-TOLUSCAD	-5.811	-1.688	4.123	2.061	3.749	3.409	1.919
$p\text{-TOLUSCAD-}H^+$	-9.894	-6.523	3.371	1.686	8.209	19.989	3.281
Aqueous Acidic medium							
SEMISCAD	-6.134	-1.790	4.344	2.172	3.962	3.614	7.663
$SEMISCAD\text{-}H^+$	-7.375	-3.539	3.836	1.918	5.457	7.764	7.919
p-TOLUSCAD	-6.069	-1.884	4.185	2.092	3.976	3.778	2.867
$p\text{-TOLUSCAD-}H^+$	-6.862	-3.262	3.600	1.800	5.062	7.117	4.409

The order of decreasing value of E_{HOMO} is *p*-TOLUSCAD > SEMISCAD for both the neutral and protonated species, both in the gas phase and in the modelled acidic medium (Table 8). This aligns with the ranking of the observed inhibition efficiencies which can be attributed to the presence of more than one aromatic ring in *p*-TOLUSCAD. Of course, this is not unexpected since iminium compounds containing aromatic rings generally exhibit high inhibition potentials to an extent that depends on the number of rings present [49].

HOMO-LUMO energy gap (ΔE) is a parameter that gives information on the overall stability/reactivity of a molecule from quantum chemical perspective. The smaller the ΔE, the higher the reactivity. In this regard, the protonated species appear to be generally more reactive than the neutral forms of the molecules. Global hardness (η) provides information on the resistivity of a molecule to change in electron density and/or electronic configuration. The higher the hardness of a molecule (i.e. the higher the value of η), the lower its reactivity and *vice versa*. On the other hand, electronegativity (χ) provides insight on the ability of a molecule to keep its electrons to itself and prevent them from being released to an acceptor. A molecule with high value of χ would not release its electrons readily to an acceptor. More so, electrophilicity (ω) can be described as a measure of the affinity of a molecule for an incoming electron. Low electrophilicity value suggests small electrophilic character but high nucleophilic behavior.

Comparing the studied inhibitors on the basis of energy gap, hardness and electronegativity, and using the protonated forms of the molecules in acidic medium (since it represents the experimental condition better), it is evident from Table 8 that $[p\text{-TOLUSCAD-H}]^+$ is softer, more reactive and less electronegative than $[SEMISCAD\text{-H}]^+$. This suggests that *p*-TOLUSCAD is more predisposed to donor-acceptor interaction with mild steel (i.e. Fe) compared to SEMISCAD, which is in tandem with the trend of inhibition efficiencies

observed from the experiments. The overall view of electrophilicity values in Table 8 suggests that [*p*-TOLUSCAD-H]$^+$ is more nucleophilic, that is, has the potential to attack a positively charged centre (like Fe surface saturated with positively charged ions) more than [SEMISCAD-H]$^+$.

3.6. Monte Carlo Simulations

In the recent time, molecular dynamic simulation has been identified as a powerful and reliable theoretical approach to investigating the adsorption behavior of inhibitor molecules on mild steel surfaces [1,16]. It helps in visualizing possible changes in the configuration, orientation and even some geometrical properties of the molecules upon adsorption thereby providing more insights on the adsorption strength and mechanism.

In the present study, the adsorption of SEMISCAD and *p*-TOLUSCAD on Fe(110) cleaved surface are investigated by Monte Carlo Simulations and the equilibrium configurations of the adsorbed molecules are shown from the side view in Figure 10. It is apparent from the figure that the molecules adsorbed in near-flat orientation on the Fe surface, which is favorable to the protection of the metallic surface. The adsorption energies (E_{ads}) shown in the figure were calculated using the equation:

$$E_{ads} = E_{[Fe-inh]} - (E_{Fe} + E_{inh}) \quad (15)$$

where $E_{[Fe\text{-}inh]}$ is the total energy of the optimized Fe/inhibitor complex, E_{Fe} is the energy of the optimized Fe(110) substrate and E_{inh} is the energy of the optimized inhibitor molecule.

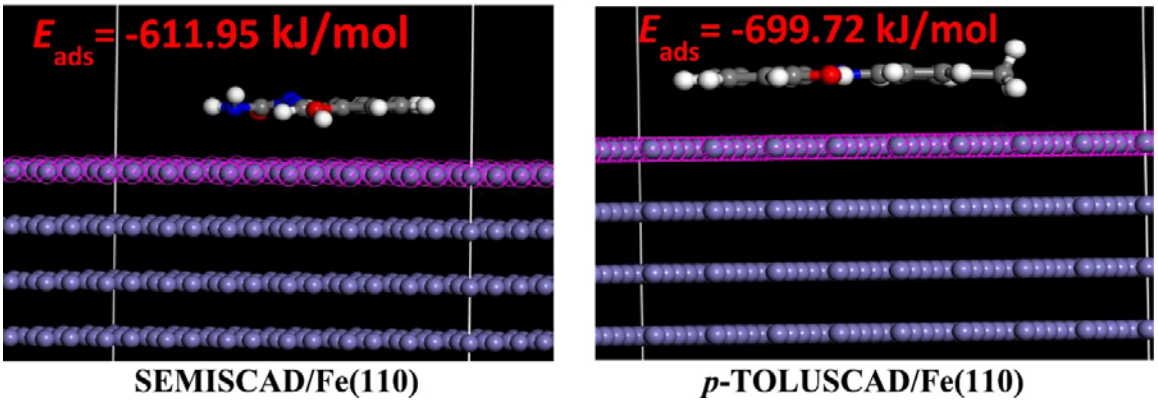

Figure 10. Equilibrium Configurations of p-TOLUSCAD/Fe(110) and SEMISCAD/Fe(110).

A large negative value of E_{ads} indicates a strong and spontaneous adsorption on the metallic surface, and the larger the negative value, the more the strength and spontaneity of the process. Thus, the values of E_{ads} obtained for the two systems (Figure 10) suggest that the adsorption of the molecules on Fe(110) surface is strong and spontaneous, but that the molecule of *p*-TOLUSCAD adsorbs better on the surface than SEMISCAD molecule. This observation is in agreement with the trend of inhibition efficiencies obtained from the experimental studies.

4. Proposed Inhibition Mechanism

A number of factors determine the mode of actions of organic compounds in inhibiting metal corrosion. These include the surface charge of the metal in an electrolyte, which invariably depends on the potential of zero charge (PZC), the type of heteroatoms or lone-pair electrons in the inhibitor molecule, and the proton affinity of the inhibitor molecule [50]. Two major modes of adsorption have been widely proposed for inhibition of steel corrosion in acid by organic compounds [51]. Neutral molecules of the inhibitor may be adsorbed on the steel surface via sharing of lone-pair electrons on the heteroatoms with the vacant d-orbitals of Fe, or donor-acceptor interactions between the pi-electrons of inhibitor molecules and d-orbitals of Fe, leading to chemical adsorption. On the other hand, it had been proven that steel surface becomes positively charged when immersed in acidic solution, such that adsorption of protonated organic base molecules could be facilitated by electrostatic interactions with chloride ions at/near the steel surface [50], [51], [52], leading to physisorption mechanism.

In the present study, the values of Gibb's free energy of adsorption derived from the experimental data (*vide supra* Table 4) suggest that the adsorption of SEMISCAD and p-TOLUSCAD molecules on mild steel surface in 1 M HCl involves both physisorption and chemisorption mechanisms. Though the decrease in inhibition efficiency with increasing temperature (*vide supra* Fig. 2) suggests physisorption mechanism [51], the fact that quantum chemically derived reactivity indices for both the neutral and protonated forms of the molecules agree with the order of inhibition efficiencies also points at the possibility of dual mechanisms, involving both neutral and charged inhibitor molecules.

In the instance of chemisorption, the neutral molecules of the Schiff bases tend to donate the lone-pair electrons on heteroatoms (e.g. N-atom of the >C=N group) to the vacant d-orbitals of Fe. The inhibitor molecules can as well establish covalent bond with Fe via the pi-electrons network, involving forward and retro/back-donations [53]. Since the Schiff bases can readily be protonated in the acid, and the steel surface is essentially positively charged in the acid, relative to the potential of zero charge, it is expected that negatively charged chloride ions will be electrostatically driven to the positively charged steel surface. The protonated inhibitor molecules, that is $[SEMISCAD\text{-}H]^+$ and $[p\text{-}TOLUSCAD\text{-}H]^+$ can then be adsorbed on the chloride layer via electrostatic interactions between oppositely charged ions. This mechanism is depicted as shown in Figure 11.

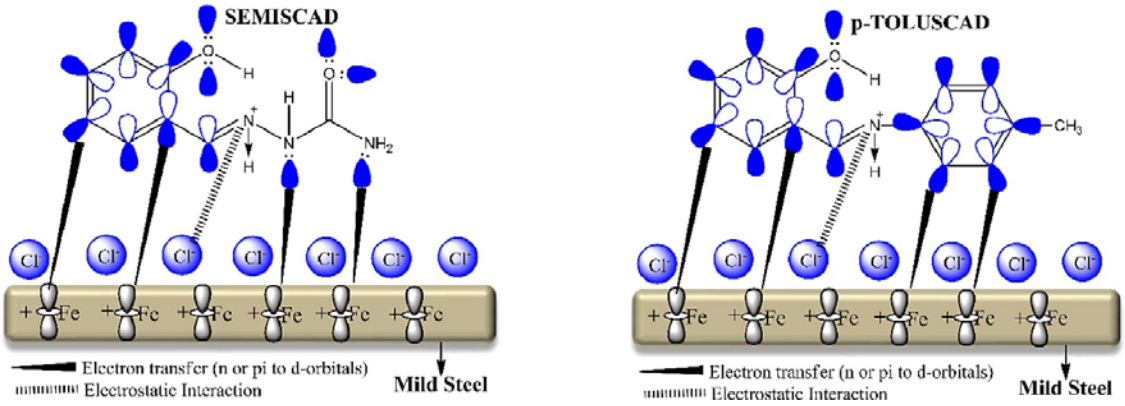

Figure 11. Images that depict the mechanism of adsorption of SEMISCAD (left-hand side) and p-TOLUSCAD (right-hand side) on mild steel surface.

5. Conclusion

Semicarbazide and *p*-toluidine derivatives of salicylic aldehyde have been synthesized and characterized using FTIR, ^{1}HNMR and ^{13}CNMR as well as melting point. The inhibitive properties of these compounds on mild steel corrosion in 1 M HCl have also been investigated using gravimetric analysis, electrochemical studies, quantum chemical calculations and molecular dynamic simulations. The following conclusions were drawn from the study:

1. SEMISCAD and *p*-TOLUSCAD were successfully synthesized as suggested by the characterization results.
2. Both compounds showed substantial inhibitive activities for mild steel corrosion in 1 M HCl solution. Their inhibition efficiencies increased with increasing concentration.
3. The studied compounds inhibit both anodic mild steel dissolution and cathodic hydrogen gas evolution reaction.
4. The compounds adsorbed at electrode (steel)/electrolyte (acid) interface to form pseudocapacitive protective film and mitigate charge transfer across the interface.
5. Experimental data for the adsorption of the studied molecules at steel/HCl interface fitted into the Temkin isotherm model, and the process was suspected to involve both physical and chemical adsorption mechanisms.
6. The inhibition potentials of p-TOLUSCAD compared to SEMISCAD might be as a result of its higher electron-donating ability, and the protonated forms of the molecules are mostly likely involved in adsorption at steel/HCl interface.
7. Experimental results are corroborated by both the DFT calculations and Monte Carlo simulations results.

Declaration of Competing Interest

Authors declare no conflict of interest on this work.

Acknowledgement

E.E.E. acknowledges the National Research Foundation (NRF) of South Africa for incentive funding for rated researchers. The authors also acknowledge the Centre for High Performance and Computing (CHPC), CSIR, South Africa for granting access to the CHPC computing resources (for the use Gaussian 09 and Materials Studio 2018 softwares). The authors thank Dr. B.A. Taleatu of the Department of Physics, Faculty of Science, Obafemi Awolowo University for granting access to the CorrTest Potentiostat.

References

[1] L.O. Olasunkanmi, I.B. Obot, M.M. Kabanda, E.E. Ebenso, Some quinoxalin-6-yl derivatives as corrosion inhibitors for mild steel in hydrochloric acid: experimental and theoretical studies, *The Journal of Physical Chemistry C* 119 (2015) 16004–16019.

[2] L.O. Olasunkanmi, M.M. Kabanda, E.E. Ebenso, Quinoxaline derivatives as corrosion inhibitors for mild steel in hydrochloric acid medium: Electrochemical and quantum chemical studies, *Physica E: Low-dimensional Systems and Nanostructures* 76 (2016) 109–126.

[3] L.C. Murulana, A.K. Singh, S.K. Shukla, M.M. Kabanda, E.E. Ebenso, Experimental and quantum chemical studies of some bis (trifluoromethyl-sulfonyl) imide imidazolium-based ionic liquids as corrosion inhibitors for mild steel in hydrochloric acid solution, *Industrial & Engineering Chemistry Research* 51 (2012) 13282–13299.

[4] J. Fu, H. Zang, Y. Wang, S. Li, T. Chen, X. Liu, Experimental and theoretical study on the inhibition performances of quinoxaline and its derivatives for the corrosion of mild steel in hydrochloric acid, *Industrial & Engineering Chemistry Research* 51 (2012) 6377–6386.

[5] E.E. Ebenso, M.M. Kabanda, L.C. Murulana, A.K. Singh, S.K. Shukla, Electrochemical and quantum chemical investigation of some azine and thiazine dyes as potential corrosion inhibitors for mild steel in hydrochloric acid solution, *Industrial & Engineering Chemistry Research* 51 (2012) 12940–12958.

[6] K.O. Sulaiman, A.T. Onawole, Quantum chemical evaluation of the corrosion inhibition of novel aromatic hydrazide derivatives on mild steel in hydrochloric acid, *Computational and Theoretical Chemistry* 1093 (2016) 73–80.

[7] N. Soltani, M. Behpour, S. Ghoreishi, H. Naeimi, Corrosion inhibition of mild steel in hydrochloric acid solution by some double Schiff bases, *Corrosion Science* 52 (2010) 1351–1361.

[8] M. Hegazy, A.M. Hasan, M. Emara, M.F. Bakr, A.H. Youssef, Evaluating four synthesized Schiff bases as corrosion inhibitors on the carbon steel in 1 M hydrochloric acid, *Corrosion Science* 65 (2012) 67–76.

[9] J.B. LI, J.E. ZUO, Influences of temperature and pH value on the corrosion behaviors of X80 pipeline steel in carbonate/bicarbonate buffer solution, *Chinese Journal of Chemistry* 26 (2008) 1799–1805.

[10] R. Samosir, S.L. Simanjuntak, *The influence of concentration and pH on corrotion rate in stainless steels–316 solution HNO3 medium*, (2017).

[11] V.S. Saji, A Review on Recent Patents in Corrosion Inhibitors, *Recent Patents on Corrosion Science*, 2010.

[12] N.O. Eddy, H. Momoh-Yahaya, E.E. Oguzie, Theoretical and experimental studies on the corrosion inhibition potentials of some purines for aluminum in 0.1 M HCl, *Journal of Advanced Research* 6 (2015) 203–217.

[13] S. Saravanamoorthy, S. Velmathi, Physiochemical interactions of chiral Schiff bases on high carbon steel surface: Corrosion inhibition in acidic media, *Progress in Organic Coatings* 76 (2013) 1527–1535.

[14] G. Gece, Drugs: a review of promising novel corrosion inhibitors, *Corrosion Science* 53 (2011) 3873–3898.

[15] S.E. Manahan, *Fundamentals of environmental chemistry*, (1993).

[16] M. El Faydy, R. Touir, M.E. Touhami, A. Zarrouk, C. Jama, B. Lakhrissi, L. Olasunkanmi, E. Ebenso, F. Bentiss, Corrosion inhibition performance of newly synthesized 5-alkoxymethyl-8-hydroxyquinoline derivatives for carbon steel in 1 M HCl solution:

experimental, DFT and Monte Carlo simulation studies, *Physical Chemistry Chemical Physics* 20 (2018) 20167–20187.

[17] P.B. Raja, M.G. Sethuraman, Natural products as corrosion inhibitor for metals in corrosive media—a review, *Materials Letters* 62 (2008) 113–116.

[18] S.K. Shukla, M. Quraishi, Cefalexin drug: A new and efficient corrosion inhibitor for mild steel in hydrochloric acid solution, *Materials Chemistry and Physics* 120 (2010) 142–147.

[19] E. Bardal, *Corrosion and protection*, Springer Science & Business Media (2007).

[20] C.M. Da Silva, D.L. da Silva, L.V. Modolo, R.B. Alves, M.A. de Resende, C. V. Martins, ˆA. de F´atima, Schiff bases: A short review of their antimicrobial activities, *Journal of Advanced Research* 2 (2011) 1–8.

[21] W. Al Zoubi, Biological activities of Schiff bases and their complexes: a review of recent works, *International Journal of Organic Chemistry* 2013 (2013).

[22] K.C. Emregül, O. Atakol, Corrosion inhibition of mild steel with Schiff base compounds in 1 M HCl, *Materials Chemistry and Physics* 82 (2003) 188–193.

[23] H. ZHANG, Y. XIE, Y. LIU, Z. YANG, Inhibition of Mild Steel Corrosion in Hydrochloric Acid Solution by Salicylaldehyde Thiosemicarbazone, *Chinese Journal of Applied Chemistry* 32 (2015) 720–725.

[24] B. Liu, H. Xi, Z. Li, Q. Xia, Adsorption and corrosion-inhibiting effect of 2-(2-{[2-(4-Pyridylcarbonyl) hydrazono] methyl} phenoxy) acetic acid on mild steel surface in seawater, *Applied Surface Science* 258 (2012) 6679–6687.

[25] M. Abdallah, H. Megahed, M. Radwan, E. Abdfattah, Polyethylene glycol compounds as corrosion inhibitors for aluminium in 0.5 M hydrochloric acid solutions, *Journal of American Science* 8 (2012) 49–55.

[26] S. Kharchouf, L. Majidi, M. Bouklah, B. Hammouti, A. Bouyanzer, A. Aouniti, Effect of three 2-allyl-p-mentha-6, 8-dien-2-ols on inhibition of mild steel corrosion in 1 M HCl, *Arabian Journal of Chemistry* 7 (2014) 680–686.

[27] M. Frisch, G. Trucks, H. Schlegel, G. Scuseria, M. Robb, J. Cheeseman, G. Scalmani, V. Barone, B. Mennucci, G. Petersson, Gaussian 09, Revision B. 01; Wallingford, CT, 2009, There is no corresponding record for this reference.[Google Scholar], (2013).

[28] H. Jacobsen, L. Cavallo, Re-evaluation of the Mn (salen) Mediated Epoxidation of Alkenes by Means of the B3LYP* Density Functional, *Physical Chemistry Chemical Physics* 6 (2004) 3747–3753.

[29] O.O. Wahab, L.O. Olasunkanmi, K.K. Govender, P.P. Govender, Synergistic effect of opposite polar substituents on selected properties of disperse yellow 119 dye, *Chemical Physics Letters* 704 (2018) 55–61.

[30] O.O. Wahab, L.O. Olasunkanmi, K.K. Govender, P.P. Govender, Tuning the aqueous solubility, chemical reactivity and absorption wavelength of azo dye systematic adjustment of molecular charge density: a DFT study, *Molecular Physics* (2019) 1–21.

[31] A.B. Anderson, S. Mehandru, Acetylene adsorption to Fe (100),(110), and (111) surfaces; structures and reactions, *Surface Science* 136 (1984) 398–418.

[32] L. Xu, D. Kirvassilis, Y. Bai, M. Mavrikakis, Atomic and molecular adsorption on Fe (110), *Surface Science* 667 (2018) 54–65.

[33] P. Noblía, E.J. Baran, L. Otero, P. Draper, H. Cerecetto, M. Gonz´alez, O.E. Piro, E. E. Castellano, T. Inohara, Y. Adachi, New Vanadium (V) Complexes with Salicylaldehyde Semicarbazone Derivatives: Synthesis, Characterization, and in vitro Insulin-Mimetic Activity-Crystal Structure of [VvO2 (salicylaldehyde semicarbazone)] *European Journal of Inorganic Chemistry*, 2004 (2004), pp. 322-328.

[34] A. Gulea, D. Poirier, J. Roy, V. Stavila, I. Bulimestru, V. Tapcov, M. Birca, L. Popovschi, In vitro antileukemia, antibacterial and antifungal activities of some 3d metal complexes: Chemical synthesis and structure–activity relationships, *Journal of Enzyme Inhibition and Medicinal Chemistry* 23 (2008) 806–818.

[35] M. Gupta, A. Sachan, S. Pandeya, V. Gangwar, Synthesis and antibacterial activity of semicarbazones and thiosemicarbazones, *Asian Journal of Chemistry* 19 (2007) 5.

[36] J.S. Bennett, K.L. Charles, M.R. Miner, C.F. Heuberger, E.J. Spina, M.F. Bartels, T. Foreman, Ethyl lactate as a tunable solvent for the synthesis of aryl aldimines, *Green Chemistry* 11 (2009) 166–168.

[37] X. Huang, Y. He, Z. Chen, C. Hu, Colorimetric sensors for anion recognition based on the proton transfer signaling mechanism, *Chinese Journal of Chemistry* 27 (2009) 1526–1530.

[38] G. Alesso, M. Sanz, M.E. Mosquera, T. Cuenca, Monocyclopentadienyl Phenoxido–Amino and Phenoxido–Amido Titanium Complexes: Synthesis, Characterisation, and Reactivity of Asymmetric Metal Centre Derivatives, *European Journal of Inorganic Chemistry* 2008 (2008) 4638–4649.

[39] Y.M. Al-Kahraman, H. Madkour, D. Ali, M. Yasinzai, Antileishmanial, antimicrobial and antifungal activities of some new aryl azomethines, *Molecules* 15 (2010) 660–671.

[40] H. Zarrok, H. Oudda, A. Zarrouk, R. Salghi, B. Hammouti, M. Bouachrine, Weight loss measurement and theoretical study of new pyridazine compound as corrosion inhibitor for C38 steel in hydrochloric acid solution, *Der Pharma Chemica* 3 (2011) 576–590.

[41] M.E. Mashuga, L.O. Olasunkanmi, A.S. Adekunle, S. Yesudass, M.M. Kabanda, E. E. Ebenso, Adsorption, thermodynamic and quantum chemical studies of 1-hexyl-3-methylimidazolium based ionic liquids as corrosion inhibitors for mild steel in HCl, *Materials* 8 (2015) 3607–3632.

[42] S.A. El Rehim, S. Sayyah, M. El-Deeb, S. Kamal, R. Azooz, Adsorption and corrosion inhibitive properties of P (2-aminobenzothiazole) on mild steel in hydrochloric acid media, *International Journal of Industrial Chemistry* 7 (2016) 39–52.

[43] C. Lai, B. Xie, L. Zou, X. Zheng, X. Ma, S. Zhu, Adsorption and corrosion inhibition of mild steel in hydrochloric acid solution by S-allyl-O, O′-dialkyldithiophosphates, *Results in Physics* 7 (2017) 3434–3443.

[44] W. Zhang, H.J. Li, Y. Wang, Y. Liu, Y.C. Wu, Adsorption and corrosion inhibition properties of pyridine-2-aldehyde-2-quinolylhydrazone for Q235 steel in acid medium: Electrochemical, thermodynamic, and surface studies, *Materials and Corrosion* 69 (2018) 1638–1648.

[45] M. Chevalier, F. Robert, N. Amusant, M. Traisnel, C. Roos, M. Lebrini, Enhanced corrosion resistance of mild steel in 1 M hydrochloric acid solution by alkaloids extract from Aniba rosaeodora plant: Electrochemical, phytochemical and XPS studies, *Electrochimica Acta* 131 (2014) 96–105.

[46] I. Benmahammed, T. Douadi, S. Issaadi, M. Al-Noaimi, S. Chafaa, Heterocyclic Schiff bases as corrosion inhibitors for carbon steel in 1 M HCl solution: hydrodynamic and synergetic effect, *Journal of Dispersion Science and Technology* (2019) 1–20.

[47] D.K. Singh, E.E. Ebenso, M.K. Singh, D. Behera, G. Udayabhanu, R.P. John, Non-toxic Schiff bases as efficient corrosion inhibitors for mild steel in 1 M HCl: Electrochemical, AFM, FE-SEM and theoretical studies, *Journal of Molecular Liquids* 250 (2018) 88–99.

[48] A. Dutta, S.K. Saha, P. Banerjee, A.K. Patra, D. Sukul, Evaluating corrosion inhibition property of some Schiff bases for mild steel in 1 M HCl: competitive effect of the heteroatom and stereochemical conformation of the molecule, *RSC Advances* 6 (2016) 74833–74844.

[49] P.R. Roberge, *Handbook of corrosion engineering*, McGraw-Hill, 2000.

[50] M. Lebrini, M. Lagrenee, H. Vezin, L. Gengembre, F. Bentiss, Electrochemical and quantum chemical studies of new thiadiazole derivatives adsorption on mild steel in normal hydrochloric acid medium, *Corrosion Science* 47 (2005) 485–505.

[51] M.A. Ibraheem, A.E.A. El Sayed Fouda, M.T. Rashad, F. Nagy Sabbahy, Sweet Corrosion Inhibition on API 5L-B Pipeline Steel, *International Scholarly Research Notices* 2012 (2012).

[52] V. Sivakumar, K. Velumani, S. Rameshkumar, Colocid dye-a potential corrosion inhibitor for the corrosion of mild steel in acid media, *Materials Research* 21 (2018).

[53] R.K. Hocking, E.C. Wasinger, Y.-L. Yan, F.M. deGroot, F.A. Walker, K.O. Hodgson, B. Hedman, E.I. Solomon, Fe L-edge X-ray absorption spectroscopy of low-spin heme relative to non-heme Fe complexes: Delocalization of Fe d-electrons into the porphyrin ligand, *Journal of the American Chemical Society* 129 (2007) 113–125.